

RSC Advances



This is an *Accepted Manuscript*, which has been through the Royal Society of Chemistry peer review process and has been accepted for publication.

Accepted Manuscripts are published online shortly after acceptance, before technical editing, formatting and proof reading. Using this free service, authors can make their results available to the community, in citable form, before we publish the edited article. This *Accepted Manuscript* will be replaced by the edited, formatted and paginated article as soon as this is available.

You can find more information about *Accepted Manuscripts* in the [Information for Authors](#).

Please note that technical editing may introduce minor changes to the text and/or graphics, which may alter content. The journal's standard [Terms & Conditions](#) and the [Ethical guidelines](#) still apply. In no event shall the Royal Society of Chemistry be held responsible for any errors or omissions in this *Accepted Manuscript* or any consequences arising from the use of any information it contains.

1 ***In vitro* and *in vivo* study of a colon-targeting resin microcapsule loading a novel**
2 **prodrug, 3, 4, 5-tributyryl shikimic acid**

3

4 Kai Dong^{1*}, Aiguo Zeng^{1*}, Maoling Wang², Yalin Dong³, Ke Wang¹, Chenning Guo¹,
5 Yan Yan¹, Lu Zhang¹, Xianpeng Shi¹, Jianfeng Xing^{1#}

6

7 ¹School of Pharmacy, Xi'an Jiaotong University, Xi'an, Shaanxi, China

8 ²Qilu Hospital of Shandong University, Qingdao, Shandong, China

9 ³Department of Pharmacy, the First Affiliated Hospital of Medical College, Xi'an
10 Jiaotong University, Xi'an, Shaanxi, China

11

12 *These authors contributed to the work equally and should be regarded as co-first
13 authors

14

15 **#Corresponding Author:** Jianfeng Xing

16 Jianfeng Xing, Ph.D.

17 School of Pharmacy, Xi'an Jiaotong University, 76 Yanta West Road, Xi'an 710061,
18 Shaanxi, China

19 Tel: +86-29-82655139 Fax: +86-29-82655139

20 E-mail: xajdxjf@mail.xjtu.edu.cn

21

22

23

24

25

26

27

28

29

30

31 **Abstract**

32

33 Prodrugs synthesized by different drugs not only overcome the defects of original
34 drugs, but also significantly enhance their treatment effects. In this study, a novel
35 prodrug, 3, 4, 5-tributyryl shikimic acid (TBS), for the treatment of ulcerative colitis
36 (UC) was synthesized by shikimic acid (SA) and butyric acid (BA) through the
37 esterification reaction. Furthermore, the anion exchange resin, Amberlite 717 was
38 employed to load the sodium salt of TBS through a batch process. Then the
39 drug-loaded exchange resin (TBSS-IER) was encapsulated in the coating material,
40 Eudragit S100, to prepare the colon-targeting drug resin microcapsule (TBSS-DRM)
41 through an in-liquid drying method. The morphology and structure of TBSS-IER and
42 TBSS-DRM were characterized by scanning electron microscopy (SEM). The *in vitro*
43 release study demonstrated the good colon-targeting of TBSS-DRM. In the *in vivo*
44 study, the TBSS-DRM exhibited good therapeutic effect on the experimental colitis
45 mouse induced by 2, 4, 6-trinitrobenzenesulfonic acid (TNBS). All results indicated
46 that the prodrug was effective for colitis and the resin microcapsule system had good
47 colon-targeting and could be used for the development of colon-targeting
48 preparations.

49

50 **Keywords:** Ulcerative colitis; Prodrugs; Shikimic acid; Butyric acid; Anion exchange
51 resin; Colon-targeting; Corticosteroids

52

53

54

55

56

57

58

59

60

61 **1. Introduction**

62

63 Ulcerative colitis (UC) is a representative type of inflammatory bowel disease and its
64 pathogenesis still remains unknown.¹⁻³ UC has a long course of disease and is prone
65 to recur, thus seriously affecting the quality of patients' life. Currently, medication is
66 still the main therapeutic regimen of UC. Generally, the drugs used for the treatment
67 of UC include corticosteroids and aminosalicyclic acids. However, some of them
68 often induced incidences of serious side-effects.^{4,5} Nowadays, many researchers are
69 pursuing potent novel drugs for UC management and many papers have reported that
70 some components of vegetables and herbs can inhibit the inflammatory response and
71 show new potential therapeutics for UC.⁶⁻⁸

72 Shikimic acid (3, 4, 5-trihydroxy-1-cyclohexene-1-carboxylic acid; SA) which is
73 extracted from the fruits of Chinese star anise (*Illicium verum* Hook. fil.) can be used
74 to improve the symptoms of UC because of its good anti-inflammation and
75 anti-coagulation effects.^{9,10} Butyric acid (BA) is a short chain fatty acid and plays an
76 important role in human body.¹¹⁻¹³ Many experiments have confirmed that BA had
77 good anti-inflammatory and therapeutic effects on UC.^{14,15} But its relatively short
78 half-life of oral administration limits its application. In this study, we synthesized a
79 novel prodrug, 3, 4, 5-tributyryl shikimic acid (TBS), through the formation of ester
80 bond between SA and BA for the treatment of UC. However, from the *in vivo*
81 experiment on mice, we found that the prodrug was easy to be hydrolyzed in the
82 upper gastrointestinal tract. So it was necessary to design a colon-targeting
83 preparation to transport the prodrug to the colon to prevent its hydrolysis in the upper
84 gastrointestinal tract and paly a better treatment role.

85 Ion-exchange resin (IER) is a kind of water insoluble inert polymer material
86 which has been widely used in several scientific investigations due to its ion-exchange
87 reaction with external-ions through their own functional groups.¹⁶⁻¹⁸ In recent years,
88 IER has been employed as a drug carrier in a variety of drug delivery systems for the
89 aims of improving effectiveness and safety of drugs, site-specific releasing,
90 taste-masking and prolonging the duration of drug action.¹⁹⁻²⁶ In this study, the

91 anion-exchange resin, Amberlite 717 was employed as the carrier to load TBS
92 through the ion-exchange reaction. Simultaneously, in order to prevent the
93 drug-loaded resin from releasing drug at the site of high ionic strength (e.g., the
94 stomach), the enteric coating material, Eudragit S100, was introduced to encapsulate
95 the drug-loaded resin to form the drug-loaded resin microcapsule. The microcapsule
96 hardly released drug in the upper gastrointestinal tract. However, in the lower
97 gastrointestinal tract, it could release drug in the colon environment of low ionic
98 strength through the degradation of Eudragit S100, thus achieving the aim of
99 colon-targeting.

100

101 **2. Materials and methods**

102

103 *2.1 Materials and reagents*

104 Shikimic acid (SA, purity>98%) was purchased from Shaanxi Sciphar Biotechnology,
105 China. Butyric acid (BA) was purchased from Shanghai Aladdin Chemistry, China.
106 717 anion-exchange resin (Amberlite 717) was obtained from Xi'an LanXiao
107 Technology, China. Eudragit S100 was purchased from Rohm, German. Liquid
108 paraffin, Span 80, PEG 400 and PEG 4000 were purchased from Tianjin Kermel
109 Chemical, China. All other reagents were analytical grade and obtained from
110 commercially available sources.

111 2, 4, 6-Trinitrobenzenesulfonic acid (TNBS) was purchased from Sigma, USA.
112 *O*-dianisidine dihydrochloride (ODD) and ethylenediaminetetraacetic acid (EDTA)
113 were purchased from Shanghai Aladdin Chemistry, China. Hexadecyl trimethyl
114 ammonium bromide (HTAB) and 30 % H₂O₂ solution were purchased from Tianjin
115 Kermel Chemical, China. All other chemicals were analytical grade, commercially
116 available products.

117

118 *2.2 Animals*

119 Male BALB/c mice weighing 20±2 g were purchased from the Laboratory Animal
120 Center of Xi'an Jiaotong University, and housed under controlled temperature and

121 relative humidity conditions of 20-25°C, and 50-60%, respectively, and under a 12/12
122 h light/dark cycle. All animals had *ad libitum* access to water and food. And they were
123 quarantined for 1 week prior to treatment. All animal care and experimental protocols
124 complied with the guidelines of animal ethics committee at Xi'an Jiaotong University.

125

126 *2.3 Synthesis of TBS*

127 In this study, a simple but efficient esterification reaction was used to synthesize TBS.
128 Specifically, 50 g SA and 200 ml BA were added to a 1,000 ml round-bottomed flask
129 and stirred until evenly. 3 drops of 98 % concentrated sulfuric acid as catalyst was
130 added to the mixture and stirred for 10 min followed by adding 500 ml ice water to
131 the flask. After being extracted by dichloromethane, the product was loaded on a
132 silica gel open column and eluted with petroleum ether / ethyl acetate (5/1). The 3, 4,
133 5-tributyryl shikimic acid was obtained after removing solvents through flash
134 evaporation (102.64 g, yield: 93.0 %).

135 The products were characterized by ¹H NMR, infrared spectroscopy (IR) and
136 mass spectrometry (MS). ¹H NMR spectra (DMSO-d₆) were recorded on a 300 MHz
137 ¹H NMR spectrometer (Bruker, Germany). Chemical shifts (δ) were reported in ppm
138 downfield from the internal standard tetramethylsilane (TMS). The IR and MS spectra
139 were recorded with FTIR-8400S IR spectrometer (Shimadzu, Japan) and
140 GCMS-QP2010 Mass Spectrometer (Shimadzu, Japan), respectively.

141

142 *2.4 Preparation of TBSS-resin microcapsule*

143 *2.4.1 Pretreatment of ion-exchange resin (IER)*

144 In this work, Amberlite 717 which was mainly composed of styrene-divinylbenzene
145 copolymer was used to encapsulate TBS. It has quaternary ammonium cationic groups
146 and the active chloride ions. Through replacing the chloride ion which was connected
147 with quaternary ammonium groups, the drug ions could be loaded in the resin.
148 Specifically, a certain quantity of Amberlite 717 was immersed and washed in 50 °C
149 deionized water to remove water-soluble impurities, then transferred them into 95 %
150 ethanol with stirring to remove the organic impurities. After washed with deionized

151 water until no residual ethanol existed, the IER was dried under vacuum at 50 °C. The
152 pre-dried IER was immersed in 0.1 mol/l hydrochloric acid solution with constant
153 stirring for 24 h, then washed with deionized water until neutral and dried to obtain
154 the anion (Cl^-) exchange resin.

155

156 *2.4.2 Preparation of TBSS-IER complex*

157 Since IER mainly encapsulates drugs through the ion-exchange reaction, drugs which
158 can be loaded into IER must be ionized. In this study, TBS first reacted with sodium
159 hydroxide (NaOH) to obtain its sodium salt. Specifically, 21.0 g TBS was added to
160 200 ml NaOH solution (0.275 mol/l) with constant stirring, the 3, 4, 5-tributyl
161 shikimic sodium (TBSS) was obtained after extraction, filtration and drying of the
162 water-soluble product. The 3, 4, 5-tributyl shikimic sodium-loaded resin
163 (TBSS-IER) complex was prepared through a batch process. The purified IER (0.50 g)
164 was suspended in a 6.0 g/l TBSS aqueous solution under magnetic stirring at 30 °C.
165 Samples were collected from TBSS aqueous solution at each predetermined time
166 interval and determined by high-performance liquid chromatography (HPLC)
167 (Methanol: water: acetic acid 75:25:0.5, v/v, C18 BDS Hypersil, column temperature
168 30 °C, flow rate 1 ml/min, detection wavelength 254 nm, LOQ: 0.15 µg/ml). The
169 drug-loading capacity (Q) of IER was determined by the measurement of the residual
170 TBSS in solution, which was calculated according to the following equation:

$$171 \quad Q_t = V/W_R \cdot (C_0 - C_t)$$

172 where Q_t was the drug-loading capacity of resin at time t. C_0 was the initial drug
173 concentration and C_t was the drug concentration at time t. V was the volume of drug
174 solution and W_R was the quality of resin.

175

176 *2.4.3 Preparation of TBSS-resin microcapsule (TBSS-DRM)*

177 Eudragit S100 is a kind of methyl acrylic acid-methyl methacrylate copolymer. It
178 is stable in the environment below pH 7.0 and degrades at pH >7.0, thus making it a
179 suitable colon-targeting preparation.^{27, 28} In this study, in order to enhance the
180 colon-targeting of TBSS-IER, Eudragit S100 was used to encapsulate TBSS-IER and

181 the in-liquid drying process was employed to prepare the TBSS-DRM.²⁹ Specifically,
182 20 ml liquid paraffin and 2.5 ml Span 80 were mixed and stirred evenly to form the
183 continuous phase. 0.1 g Eudragit S100 and 0.01 g PEG 400 were dissolved in 7.5 ml
184 acetone to form the dispersed phase, 0.5 g TBSS-IER (containing about 0.5 g prodrug)
185 was firstly immersed in 50 ml 20 % (w/w) PEG 4000 solution and then added in the
186 dispersed phase with stirring. The prepared dispersed phase was dropped into the
187 continuous phase to form emulsion with constant stirring for 6 h at 40 °C to remove
188 acetone. The obtained TBSS-DRM was filtered and washed by petroleum ether to
189 remove liquid paraffin and dried at 40 °C.

190 The morphology of the TBSS-IER and TBSS-DRM was characterized by
191 scanning electron microscopy (SEM). The drug-loaded IER and DRM were frozen in
192 liquid nitrogen, and then lyophilized for 72 h. The lyophilized IER and DRM were
193 then sputtered with gold, and their morphology and microstructure were observed by
194 a scanning electron microscope (TM-1000, HITACHI, Japan).

195

196 *2.5 In vitro drug release study*

197 In this part, two *in vitro* release experiments were investigated according to the paddle
198 method for dissolution test in Chinese Pharmacopoeia (2010 edition), respectively.
199 The first experiment was to investigate the impact of the ionic concentration on the
200 ion-exchange ability of TBSS-IER. Specifically, 0.1 g TBSS-IER was added in three
201 sodium chloride (NaCl) solutions of different concentrations (0.05 mol/l, 0.15 mol/l
202 and 0.80 mol/l), respectively. The operation was carried under the condition of 37±0.5
203 °C and 50 rpm. 5 ml samples were collected and replaced with the same volume of
204 release medium at predetermined time intervals. The HPLC method was used to
205 determine the TBSS content in the release medium. The second experiment was to
206 investigate the release behavior of TBSS-DRM and to simulate the process of the
207 gastrointestinal transit *in vivo*. Specifically, 0.5 g TBSS-DRM was successively added
208 into artificial gastric juice (pH=1.2) for 2 h, artificial small intestinal juice (pH=6.8)
209 for 4 h and artificial colon juice (pH=7.4) for 6 h. And the operation was carried under
210 the condition of 37±0.5 °C and 50 rpm. 5 ml samples were collected and replaced with

211 the same volume of release medium at predetermined time interval (1 h). In the *in*
212 *vitro* study, the volumes of all dissolution media were 900 ml, and after filtering
213 through 0.45 μm filter membrane, samples of the two experiments were determined
214 by HPLC according to 2.4.2 section, and calculated the percentage of cumulative
215 release (%).

216

217 *2.6 Therapy of TBSS-DRM on the experimental colitis induced by TNBS in mice*

218 *2.6.1 Induction of colitis and experimental protocols*

219 Colitis was induced according to the procedure described by Wang et al.³⁰ Specifically,
220 after 12 h of fasting, mice were anesthetized with ether before induction of colitis. 0.1
221 ml 50 % (v/v) ethanol which contained 2.5 % (v/v) TNBS was instilled into the colon
222 3.5-4.0 cm from the anus by a gavage needle. Mice were kept in a head-down position
223 for 30 s to prevent the leakage of the intracolonic instillation. Mice in the control
224 group received physiological saline instead of TNBS solution. From the results of our
225 pre-experiments, TBS was undetectable in colon due to the rapid hydrolysis of the
226 ester bond in the upper gastrointestinal tract. Therefore, dexamethasone sodium
227 phosphate (DXSP), which was also used in the treatment of UC, was selected to
228 replace TBSS as the positive control. The mice were randomly divided in to 4 groups:
229 (1) control-no colitis induced (p.o., 0.5% CMC-Na, $n=15$), (2) TNBS (p.o., 0.5%
230 CMC-Na, $n=15$), (3) TNBS+DXSP (p.o., 2 mg/kg DXSP, $n=15$), (4) TNBS+TBSS
231 (p.o., 200 mg/kg TBSS, $n=15$). The treatment was given after the induction of colitis
232 for 12 h. During the experiment, the mice body weight changes of each group were
233 recorded and mice feces were collected to investigate their characteristics and
234 determine the fecal occult blood daily. At the end of the experiment, the number of the
235 ultimately surviving mice was recorded and the final survival rate was calculated.
236 Then all of the mice in the respective groups were killed, and the entire colon was
237 excised and cleaned of adherent adipose tissue, opened longitudinally, and rinsed with
238 cold physiological saline to remove fecal. The intestinal segment from each mouse
239 was stored at $-70\text{ }^{\circ}\text{C}$ for subsequent measurement.

240

241 2.6.2 Measurement of disease activity index (DAI)

242 Disease activity index (DAI) which reflects the therapeutic effect of different drugs on
243 colitis induced by TNBS is the sum of scores given for body weight loss (scored as: 0,
244 none; 1, 1-5 %; 2, 5-10 %; 3, 10-15 %; 4, over 15 %), stool consistency (scored as: 0,
245 well-formed pellets; 2, loose stools; 4, diarrhea) and fecal occult blood (scored as: 0,
246 normal; 1, occult blood+; 2, Occult blood++; 3, Occult blood+++; 4, visible blood in
247 the stool).³¹ The test of mouse fecal occult blood was performed using *o*-toluidine.
248 Specifically, a small amount of mouse feces was smeared on a white plate. 2-3 drops
249 of 10 g/l of *o*-toluidine in glacial acetic acid solution was dripped into the feces and
250 blended evenly. Then 2-3 drops of 3 % H₂O₂ solution was added in the mixture, which
251 was followed by timing as well as observing the results immediately. The evaluation
252 criteria of fecal occult blood level were shown in **Table 1**. In this study, the DAI of
253 each group were recorded daily and the figure of DAI varying trend was drawn.
254 Moreover, the differences between groups were evaluated simultaneously.

255

256 2.6.3 Measurement of MPO Activity

257 The measurement of Myeloperoxidase (MPO) is to determine the activity of
258 myeloperoxidase which is used to measure the accumulation of neutrophils.³²
259 Specifically, the weighted tissue samples were homogenized in ten volumes of
260 ice-cold phosphate buffer (50 mM K₂HPO₄, pH 6.0) containing 0.5% (w/v) HTAB.
261 The homogenate was centrifuged at 10,000 rpm for 10 min at 4 °C, and the
262 supernatant was discarded. The precipitate was then homogenized with an equivalent
263 volume of 50 mM K₂HPO₄ containing 0.5 % (w/v) HTAB and 10 mM EDTA. MPO
264 activity was assessed by measuring the hydrogen-peroxide-dependent oxidation of
265 *o*-dianisidine dihydrochloride (ODD). One enzyme unit was defined as the amount of
266 enzyme producing one absorbance change per minute at 460 nm and 37 °C. Enzyme
267 activity was calculated as U/g tissue.³³

268

269 2.7 Statistical analysis

270 Statistical analyses were performed with SPSS version 13.0 for Windows. All results

271 were expressed as mean \pm SD. Data between groups were compared using Wilcoxon
272 rank sum test. And data among multiple groups were compared using Kruskal-Wallis
273 test. $p < 0.05$ was considered to be statistically significant.

274

275 **3. Results**

276

277 *3.1 Synthesis and characterization of TBS*

278 In this study, the prodrug, 3, 4, 5-tributyryl shikimic acid was obtained through the
279 formation of ester bond between BA and SA (**Scheme 1**). The structure of TBS was
280 determined by ^1H NMR in CDCl_3 , and the spectrum was shown in **Fig.1**. Specifically,
281 the peaks at 1.0, 1.7 and 2.2 ppm belonged to the methyl group (CH_3), the β and the γ
282 methylene group (CH_2), respectively. While the peaks at 2.3, 2.8 and 5.8 ppm were
283 attributed to the methylidynes (CH) of the hexatomic ring which directly connected
284 with the BA groups. The peaks at 5.3 and 6.9 belonged to the methylene group (CH_2)
285 and the double bond of the hexatomic ring. The 7.3 ppm corresponded to the protons
286 of the carboxyl group ($-\text{COOH}$).

287 The FTIR spectra of 5-BA was shown in **Fig.2**. In general, the absorption bands
288 at 3256 cm^{-1} and 1743 cm^{-1} were attributed to the carboxyl group ($-\text{COOH}$). The peak
289 at 1697 cm^{-1} , 1250 , 1165 , 1103 cm^{-1} belonged to the ester ($\nu\text{C}=\text{O}$ and $\nu\text{C}-\text{O}-\text{C}$) formed
290 between SA and BA. Furthermore, the molecular ion peak of TBS was MS m/z 384
291 (MH^+). These results indicated that TBS was successfully synthesized through the
292 formation of the ester band between BA and SA.

293

294 *3.2 Preparation of TBSS-IER and TBSS-DRM*

295 In this work, the batch process was used to encapsulate the prodrug.³⁴ In order to be
296 encapsulated into the IER, the sodium salt of TBS (TBSS) was synthesized through a
297 simple reaction with NaOH. During the drug-loading process, samples collected at
298 each time interval were determined by HPLC. And the drug-loading capacity (Q) was
299 the difference between the total dosage and the residual TBSS in solution. **Fig.3**
300 showed the drug-loading capacity of resin changing over time. As shown in **Fig.3**, the

301 ion-exchange reaction got equilibrium at 1 h, and the drug-loading capacity was 1.07
302 g/g. In the coating process, in-liquid drying method was used to prepare TBSS-DRM.
303 Liquid paraffin which was stable and non-volatile was selected as the continuous
304 phase. The dispersed phase was acetone which could dissolve the coating material
305 (Eudragit S100) and be volatilized easily. Span 80 and PEG 400 were used as
306 emulsifier and plasticizer, respectively. Moreover, after immersing in PEG 4000
307 solution, the swelling degree of TBSS-IER significantly reduced, thus preventing the
308 burst release of TBSS after the film-coated layer (Eudragit S100) degrading. In this
309 work, the TBSS-DRM was obtained through removing the volatile dispersed phase by
310 heating and stirring, thus guaranteeing the shape of and the dispersion of TBSS-DRM.

311 The typical scanning electron microphotographs of TBSS-IER and TBSS-DRM
312 were presented in **Fig. 4**. **Fig. 4A** showed that the drug-loaded resin was a sphere, and
313 its particle size was about 600 μm . **Fig. 4B** exhibited the surface morphology of the
314 drug-loaded resin. There were numerous tiny cavities on the surface of the resin,
315 suggesting that the TBSS could enter the resin through them. **Fig. 4C** showed that,
316 after coating with Eudragit S100, the volume of the microcapsule did not change
317 obviously. Moreover, the leakage of drug caused by ion-exchange would be reduced
318 in acid environment due to the coverage of the coating material.

319

320 *3.3 In vitro drug release study*

321 **Fig.5A** showed the influence of the concentration of release medium on the release
322 behavior of TBSS-IER. With the increase of the medium concentration, the
323 percentage of cumulative release increased as well. When the concentration of NaCl
324 was 0.15 mol/l, the ultimate cumulative release percentage was almost twice of that of
325 0.05 mol/l NaCl. While the cumulative release percentage of 0.8 mol/l NaCl had no
326 significant difference with that of 0.15 mol/l, indicating that with the increase of NaCl
327 concentration, the ion-exchange capacity of resin also increased. However, when the
328 concentration reaching a certain extent (e.g., 0.15 mol/l), the ion-exchange capacity of
329 resin tended to saturation. Then the increase of ion concentration would not improve
330 the drug-loading capacity of resin. **Fig.5B** was the *in vitro* release curve of

331 TBSS-DRM at different pH values. This experiment imitated the variation of pH
332 values and the transit time of the whole gastrointestinal tract (including stomach,
333 small intestine and colon). As we know, it is desired that a colon-targeting preparation
334 hardly releases drug in the gastric environment (pH 1.2), releases parts of drug in
335 intestinal environment (pH 6.8) and releases lots of drug in the colon environment
336 (pH 7.4). And the results of the *in vitro* release experiment confirmed the good
337 colon-targeting property of TBSS-DRM. As shown in **Fig. 5B**, TBSS-DRM hardly
338 released TBSS in the acidic environment. However, its release behavior changed
339 significantly when the pH values varied. In the intestinal environment (pH 6.8), the
340 accumulative release was <30%. While in the colonic environment (pH 7.4), massive
341 TBSS released from the TBSS-DRM (>80%). This release behavior facilitated drugs
342 to be concentrated at the targeting-site and play therapeutic effects.

343

344 *3.4 Effect of TBSS-DRM on the mouse survival rate and body weight changes*

345 After 5 days of treatment, no mice died in the control group. However, 8 mice died in
346 the TNBS group. Moreover, the death number in DXSP group and TBSS-DRM group
347 was similar (5 mice died in DXSP group and 4 mice died in TBSS-DRM group),
348 which might be due to the relatively large individual differences of the resistance of
349 mouse to TNBS. **Fig. 6** presented the influence of TBSS-DRM on body weight
350 changes. From **Fig. 6**, the weight of the control group always maintained stable
351 growth. However, the TNBS group showed sharp decline, then the decreasing trend
352 slowed down. Furthermore, both weights of the TBSS-DRM group and the DXSP
353 solution group began to rise gradually from the second day after administration and
354 showed stable growth trend. However, compared with the DXSP solution group, the
355 TBSS-DRM group showed a more obvious growth trend, indicating a better
356 therapeutic effect of TBSS-DRM.

357

358 *3.5 Effect of TBSS-DRM on DAI and MPO Activity*

359 After the experimental colitis was successfully induced, the mice appeared some
360 conditions, such as bloody stools, diarrhea, reduced activity and weight loss after 24 h.

361 **Fig. 7A** reflected the variation tendency of the DAI of each group and **Fig. 7B**
362 presented the influence of TBSS-DRM on the ultimate DAI. The DAI of control
363 group was 0. However, due to the influence of inflammation, the DAI of TNBS group
364 was significantly higher than the TBSS-DRM group and DXSP solution group. After
365 treatment, both DAI of TBSS-DRM group and DXSP solution group showed obvious
366 decline. The results of **Fig. 7B** indicated that both DAI of TBSS-DRM group and
367 DXSP solution group showed significant difference compared with the TNBS group
368 ($p < 0.01$), and they both showed similar decreased trend. Moreover, **Fig. 8** showed the
369 influence of TBSS-DRM on the activity of MPO. As shown in **Fig. 8**, compared with
370 the TNBS group, MPO activity of TBSS-DRM group and DXSP solution group both
371 decreased significantly ($p < 0.01$). And the downward trend of them was similar,
372 indicating that both of them could effectively relieve the inflammation at the colon
373 site. Both results of the variation of DAI and MPO activity suggested the good
374 treatment of TBSS-DRM on the TNBS induced colitis of mice.

375

376 **4. Discussion**

377

378 Prodrug can improve the *in vivo* pharmacokinetics of the original drug including
379 absorption, distribution, metabolism and excretion through changing the physical or
380 chemical properties of the original drug by chemical modification, thereby
381 overcoming the shortcomings and enhanced the therapeutic effect of the original drug.
382 In this work, TBS was synthesized by SA and BA, and the prodrug could release SA
383 and BA through the hydrolysis of ester bond, thus playing a collaborative therapeutic
384 effect on UC. However, we found that the prodrug had poor water-solubility and was
385 easy to be hydrolyzed in the upper gastrointestinal tract after repeated experiments. So
386 we intended to use appropriate carriers to concentrate drugs to the lesion site
387 according to the variation of the *in vivo* environment (e.g., pH values, enzyme and
388 ionic strength), thus not only improving the treatment effect but also preventing
389 hydrolysis of the prodrug in advance. In this study, we used IER as the carrier to load
390 TBS through ion-exchange. Then the coating material, Eudragit S100, was used to

391 encapsulate the drug-loaded IER so that it could be targeting to the colon site
392 depending on the variation of the *in vivo* pH values. After the degradation of Eudragit
393 S100, IER could release TBS at colon through ion-exchange. Then TBS was
394 hydrolyzed and released SA and BA, thus having therapeutic effects (**Scheme 2**).

395 As a carrier, resin can load drug depending on ion-exchange and its special
396 structure. As depicted in **Fig.4**, TBSS could enter the interior of resin through these
397 cavities on the surface, then achieving the drug-loading through ion-exchange
398 reaction. Moreover, the stability of drug-loaded microcapsule in acid environment
399 could be effectively improved by coated with Eudragit S100, thereby preventing the
400 leakage of drug in the upper gastrointestinal tract. From **Fig. 3**, the drug-loading
401 capacity of resin reached saturation in a relatively short period of time (1 h, 1.07 g/g).
402 Moreover, the release behavior could be adjusted via the media concentration. In the
403 *in vitro* release study, **Fig. 5A** showed that with the increasing of the concentration of
404 NaCl solution, the release percentage of the drug-loaded resin increased accordingly.
405 The release percentage of drug-loaded resin in NaCl solutions with 0.15 and 0.8 mol/l
406 concentrations were much higher than the 0.05 mol/l solutions, indicating that the
407 release of drug-loaded resin was a concentration-dependent manner. With the increase
408 of the media concentration, the number of the anions which replaced TBSS in resin
409 increased accordingly. Therefore, more TBSS can be released. However, due to the
410 limitation of the volume and the number of active groups, the exchange capacity of
411 resin was limited. Therefore, when the medium concentration increased from 0.15
412 mol/l to 0.80 mol/l, the release percentage had very small growth and the release
413 amount got the maximum after 2 h (**Fig. 5A**). We can suppose that because the release
414 of the drug-loaded resin is mainly influenced by the ionic strength, once orally taken,
415 the resin will release drug rapidly in the strong electrolyte environment (e.g., in
416 stomach), thus failed to achieve the colon-targeting. Therefore, we employed Eudragit
417 S100 to encapsulate the TBS-IER through the in-liquid dying method to prepare the
418 TBSS-DRM. The results of **Fig. 5B** suggested that since Eudragit S100 could not
419 degrade at pH 1.2, TBSS was hardly released at this pH value. However, at pH 6.8,
420 Eudragit S100 began to degrade and the TBSS-loaded resin was gradually exposed

421 and released drugs through ion-exchange between resin and solution. At pH 7.4,
422 Eudragit S100 was completely degraded and drugs were completely released.
423 Moreover, with the gradually degradation of Eudragit S100, no burst release occurred
424 during the release of TBSS. The main reason was that, because of the ion-exchange
425 between resin and solution-ions, TBSS was gradually released. And the secondary
426 reason was the PEG 4000 which delayed the drug release. While at pH 7.4, the
427 Eudragit S100 was completely degraded and the TBSS-loaded resin was completed
428 exposed to the solution, the ionic strength around the resin significantly increased and
429 the ion-exchange degree accelerate as well. Therefore, the drug release increased
430 significantly.

431 In the *in vivo* study, the results of mice survival rate and body weight changes
432 showed that after the treatment of TBSS-DRM, both the survival rate and weight of
433 mice were increased, thus confirming the good therapeutic effect of TBS on the
434 experimental colitis. Moreover, the measurement of DAI and MPO activity also
435 indicted that TBS had good inhibitory effects on the inflammation at the colon site.
436 And there was no significant difference between the TBSS-DRM group and DXSP
437 solution group about in therapeutic effect on the TNBS induced colitis mice. However,
438 long-term or improper use of corticosteroids will cause many side-effects, such as the
439 risk of opportunistic infection, diabetes mellitus, osteoporosis and the possible
440 development of steroid-dependent disease.³⁵⁻³⁷ The TBSS-loaded resin encapsulated
441 in the coating film (Eudragit S100) and hardly released drug at lower pH values (e.g.,
442 at stomach). However, in the colon environment, due to the degradation of Eudragit
443 S100, the TBSS-loaded resin was exposed to the colon site and began to release TBSS.
444 Moreover, due to the weak electrolyte concentration and the relatively small volume
445 of colon, the exchange process of TBSS anions with external ions was relatively
446 slower and TBSS could be gradually released. Also, with the hydrolysis of SA and BA,
447 the TBSS-DRM would achieve a synergistic therapeutic effect and a sustained-release
448 action. In conclusion, this method not only avoided TBSS being hydrolyzed in the
449 upper digestive tract, but also achieved a similar therapeutic effect as corticosteroids.

450

451 **5. Conclusion**

452

453 In this study, a novel prodrug, 3, 4, 5-tributyryl shikimic acid (TBS), was synthesized
454 by SA and BA through esterification reaction. Then the prodrug was encapsulated in
455 Amberlite 717 through a batch process. Furthermore, in order to improve the
456 colon-targeting property and the therapeutic effects of TBSS-IER, the coating
457 polymer material, Eudragit S100, was employed to encapsulate TBSS-IER to prepare
458 the colon-targeting drug resin microcapsule (TBSS-DRM) through the in-liquid
459 drying process. The morphology of the TBSS-IER and TBSS-DRM were
460 characterized by SEM. The *in vitro* release study showed that the TBSS-IER exhibited
461 concentration-dependent release behavior and the TBSS-DRM displayed pH-sensitive
462 release behavior. In the *in vivo* study, due to the colon-targeting and ion-exchange
463 function, TBSS-DRM showed a similar therapeutic effect as compared with
464 dexamethasone. All results indicated that the prodrug was effective for colitis and the
465 resin microcapsule system had good colon-targeting property and could be used for
466 the development of colon-targeting preparations.

467

468 **Acknowledgement**

469 This work was financially supported by Fundamental Research Funds for the Central
470 Universities (xj08142016 and xjj2013054), China Postdoctoral Science Foundation
471 Funded Project (2014M562429) and Natural Science Foundation of China (No.
472 30973578 and No. 81473177).

473

474 **Conflicts of interests:** None declared.

475

476

477

478

479

480

481 **References**

482

- 483 1. J. Meier and A. Sturm, *World journal of gastroenterology : WJG*, 2011, **17**,
484 3204-3212.
- 485 2. H. J. Freeman, *Therapeutics and clinical risk management*, 2013, **9**, 451-456.
- 486 3. W. Blonski, A. M. Buchner and G. R. Lichtenstein, *Current opinion in*
487 *gastroenterology*, 2014, **30**, 84-96.
- 488 4. C. De Cassan, G. Fiorino and S. Danese, *Dig. Dis.*, 2012, **30**, 368-375.
- 489 5. K. Motegi, K. Nagasako, H. Nogawa, T. Akiya, Y. Kon and T. Sawada, *Nihon*
490 *rinsho. Japanese journal of clinical medicine*, 1999, **57**, 2466-2471.
- 491 6. K. Sugimoto, H. Hanai, K. Tozawa, T. Aoshi, M. Uchijima, T. Nagata and Y.
492 Koide, *Gastroenterology*, 2002, **123**, 1912-1922.
- 493 7. A. P. Bai, O. Y. Qin and R. W. Hu, *Digestive diseases and sciences*, 2005, **50**,
494 1426-1431.
- 495 8. A. R. Martin, I. Villegas, C. La Casa and C. A. de la Lastra, *Biochemical*
496 *Pharmacology*, 2004, **67**, 1399-1410.
- 497 9. A. A. Bertelli, C. Mannari, S. Santi, C. Filippi, M. Migliori and L. Giovannini,
498 *Journal of medical virology*, 2008, **80**, 741-745.
- 499 10. Y. Ma, Q. P. Xu, J. N. Sun, L. M. Bai, Y. J. Guo and J. Z. Niu, *Zhongguo Yao*
500 *Li Xue Bao*, 1999, **20**, 701-704.
- 501 11. A. de Conti, V. Tryndyak, I. Koturbash, R. Heidor, J. Kuroiwa-Trzmielina, T. P.
502 Ong, F. A. Beland, F. S. Moreno and I. P. Pogribny, *Carcinogenesis*, 2013, **34**,
503 1900-1906.
- 504 12. S. Molina, M. I. Moran-Valero, D. Martin, L. Vazquez, T. Vargas, C. F. Torres,
505 A. Ramirez de Molina and G. Reglero, *Chemistry and physics of lipids*, 2013,
506 **175-176**, 50-56.
- 507 13. A. Zaleski, A. Banaszkiwicz and J. Walkowiak, *Przegląd*
508 *gastroenterologiczny*, 2013, **8**, 350-353.
- 509 14. A. Di Sabatino, R. Morera, R. Ciccocioppo, P. Cazzola, S. Gotti, F. P. Tinozzi,
510 S. Tinozzi and G. R. Corazza, *Aliment Pharmacol Ther*, 2005, **22**, 789-794.

- 511 15. P. Vernia, G. Monteleone, G. Grandinetti, G. Villotti, E. Di Giulio, G. Frieri, A.
512 Marcheggiano, F. Pallone, R. Caprilli and A. Torsoli, *Digestive diseases and*
513 *sciences*, 2000, **45**, 976-981.
- 514 16. L. P. Amsel and O. N. Hinsvark, *Pharm Technology*, 1984, **4**.
- 515 17. V. Anand, R. Kandarapu and S. Garg, *Drug discovery today*, 2001, **17**.
- 516 18. X. Guo, R. K. Chang and M. A. Hussain, *J Pharm Sci*, 2009, **98**, 3886-3902.
- 517 19. S. Burton, N. Washington, R. J. C. Steele, R. Musson and L. Feely, *J Pharm*
518 *Pharmacol*, 1995, **47**, 901-906.
- 519 20. S. H. Jeong and K. Park, *International journal of pharmaceutics*, 2008, **353**,
520 195-204.
- 521 21. S. Narisawa, M. Nagata, C. Danyoshi, H. Yoshino, K. Murata and K. Noda,
522 *Pharmaceutical research*, 1994, **11**, 111-116.
- 523 22. W. Samprasit, P. Akkaramongkolporn, T. Ngawhirunpat, T. Rojanarata and P.
524 Opanasopit, *AAPS PharmSciTech*, 2013, **14**, 1118-1128.
- 525 23. H. Sohi, Y. Sultana and R. K. Khar, *Drug Dev Ind Pharm*, 2004, **30**, 429-448.
- 526 24. C. P. Yewale, M. N. Rathi, G. G. Kore, G. V. Jadhav and M. P. Wagh,
527 *Pharmaceutical development and technology*, 2013, **18**, 367-376.
- 528 25. L. Yu, S. Li, Y. Yuan, Y. Dai and H. Liu, *International journal of*
529 *pharmaceutics*, 2006, **319**, 107-113.
- 530 26. Y. Chen, M. A. Burton, J. P. Codde, S. Napoli, I. J. Martins and B. N. Gray, *J*
531 *Pharm Pharmacol*, 1992, **44**, 211-215.
- 532 27. S. Thakral, N. K. Thakral and D. K. Majumdar, *Expert Opin. Drug Deliv.*,
533 2013, **10**, 131-149.
- 534 28. N. K. Thakral, A. R. Ray and D. K. Majumdar, *Journal of materials science.*
535 *Materials in medicine*, 2010, **21**, 2691-2699.
- 536 29. M. Li, O. Rouaud and D. Poncelet, *International journal of pharmaceutics*,
537 2008, **363**, 26-39.
- 538 30. W. P. Wang, X. Guo, M. W. Koo, B. C. Wong, S. K. Lam, Y. N. Ye and C. H.
539 Cho, *Am J Physiol Gastrointest Liver Physiol*, 2001, **281**, G586-594.
- 540 31. S. H. Patel, M. A. Rachchh and P. D. Jadav, *Indian J Pharmacol*, 2012, **44**,

- 541 744-748.
- 542 32. A. J. McCabe, M. Dowhy, B. A. Holm and P. L. Glick, *Journal of pediatric*
543 *surgery*, 2001, **36**, 334-337.
- 544 33. A. Bozkurt, B. Cakir, F. Ercan and B. C. Yegen, *Regul. Pept.*, 2003, **116**,
545 109-118.
- 546 34. H. Ichikawa, K. Fujioka, M. C. Adeyeye and Y. Fukumori, *International*
547 *journal of pharmaceutics*, 2001, **216**, 67-76.
- 548 35. D. R. Friend, *Advanced drug delivery reviews*, 2005, **57**, 247-265.
- 549 36. R. Dahl, *Respir. Med.*, 2006, **100**, 1307-1317.
- 550 37. A. L. Buchman, *J. Clin. Gastroenterol.*, 2001, **33**, 289-294.
- 551
- 552
- 553
- 554
- 555
- 556
- 557
- 558
- 559
- 560
- 561
- 562
- 563
- 564
- 565
- 566
- 567
- 568
- 569
- 570

571 **Figure legends**

572

573 **Scheme 1** Synthesis scheme of 3, 4, 5-tributyryl shikimic acid (TBS).

574

575 **Scheme 2** Schematic preparation, administration, and *in vivo* release behavior of
576 TBSS-DRM.

577

578 **Fig.1** ^1H NMR spectrum of TBS (in CDCl_3).

579

580 **Fig.2** FTIR spectrum of TBS.

581

582 **Fig. 3** The variation of the drug-loading capacity (Q) of resin versus time during the
583 TBSS-IER preparation.

584

585 **Fig. 4** SEM images of TBSS-IER (A), the surface morphology of TBSS-IER (B) and
586 TBSS-DRM (C).

587

588 **Fig. 5** The *in vitro* release behavior of TBSS-IER in three NaCl solutions of different
589 concentrations (0.05 mol/l, 0.15 mol/l and 0.80 mol/l) (A) and TBSS-DRM in release
590 medium with different pH values (B). For figure B, The experiment was successively
591 conducted at pH 1.2 (from 0 to 2 h), pH 6.8 (from 3 to 6 h) and pH 7.4 (from 7 to 10
592 h).

593

594 **Fig. 6** The influence of TBSS-DRM and DXSP on the body weight changes of mice.
595 Data are shown as mean \pm SD, n=15.

596

597 **Fig. 7** The influence of TBSS-DRM and DXSP on the variation of DAI index of mice
598 (A) and the influence of TBSS-DRM and DXSP on the ultimate DAI index of mice
599 (B). ^{#,*}Mean values with different superscript symbols were significantly different.

600 ^{##} $p < 0.01$ compared to control group; ^{**} $p < 0.01$ compared to TNBS group. Data are

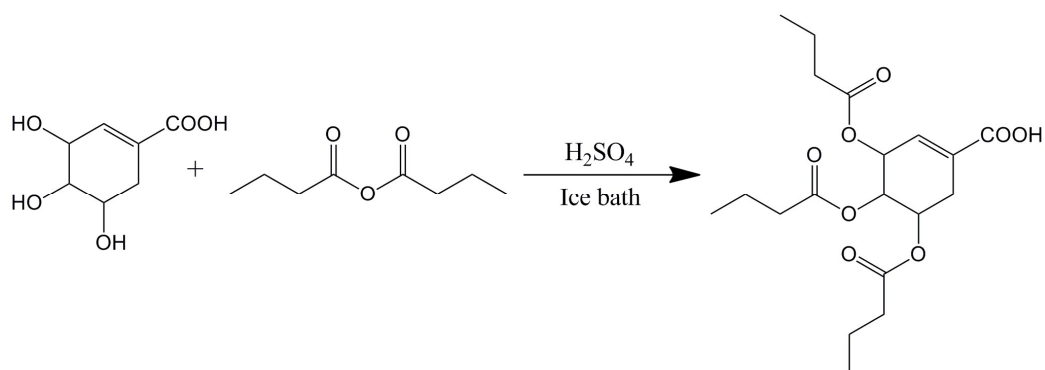
601 shown as mean \pm SD, n=15. *Control* control group, *TNBS* TNBS group, *DXSP* DXSP
602 p.o. group, *TBSS-DRM* TBSS-DRM p.o. group.

603

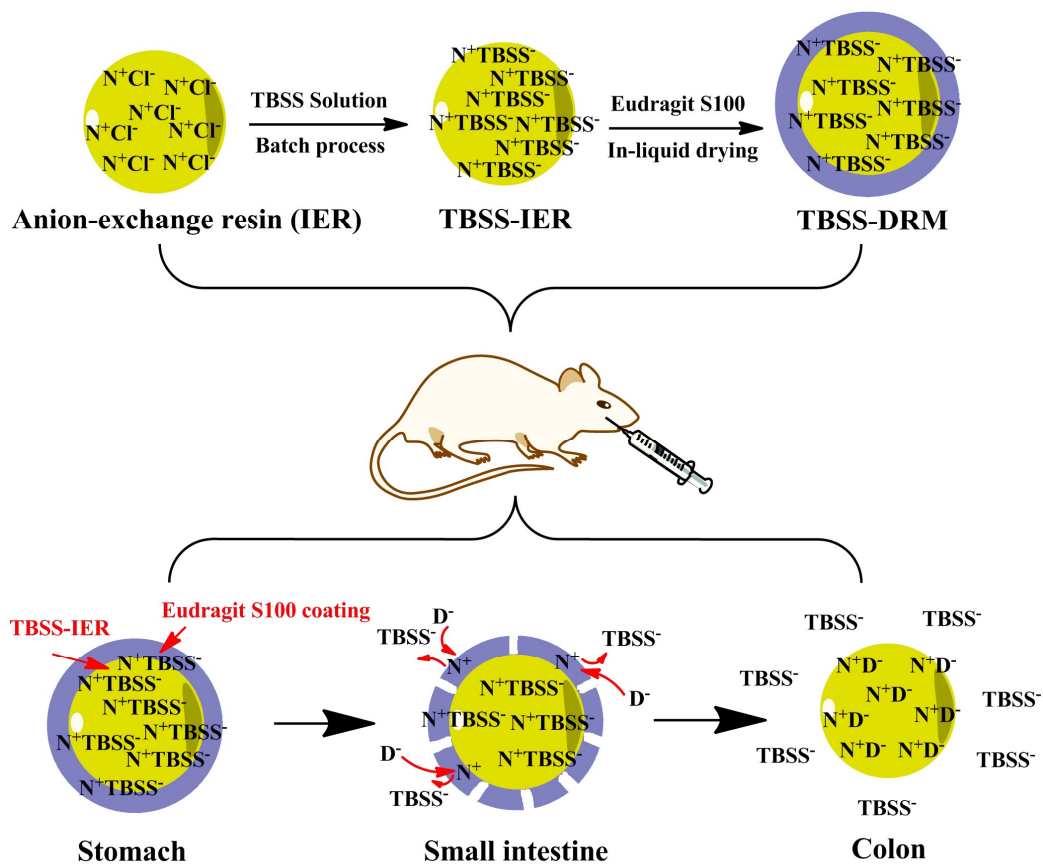
604 **Fig. 8** The influence of TBSS-DRM and DXSP on the activity of MPO in the colon
605 tissue of mice. #,*Mean values with different superscript symbols were significantly
606 different. ## $p < 0.01$ compared to control group; ** $p < 0.01$ compared to TNBS group.

607 *Control* control group, *TNBS* TNBS group, *DXSP* DXSP p.o. group, *TBSS-DRM*
608 TBSS-DRM p.o. group.

609

Figures

Scheme 1 Synthesis scheme of 3, 4, 5-tributyl shikimic acid (TBS).



Scheme 2 Schematic preparation, administration, and *in vivo* release behavior of TBSS-DRM.

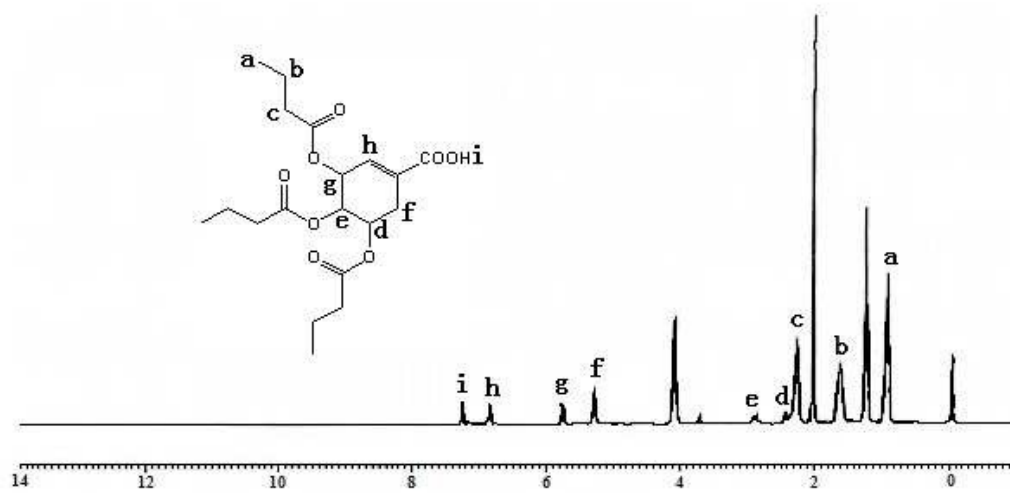


Fig.1 ¹H NMR spectrum of TBS (in CDCl₃).

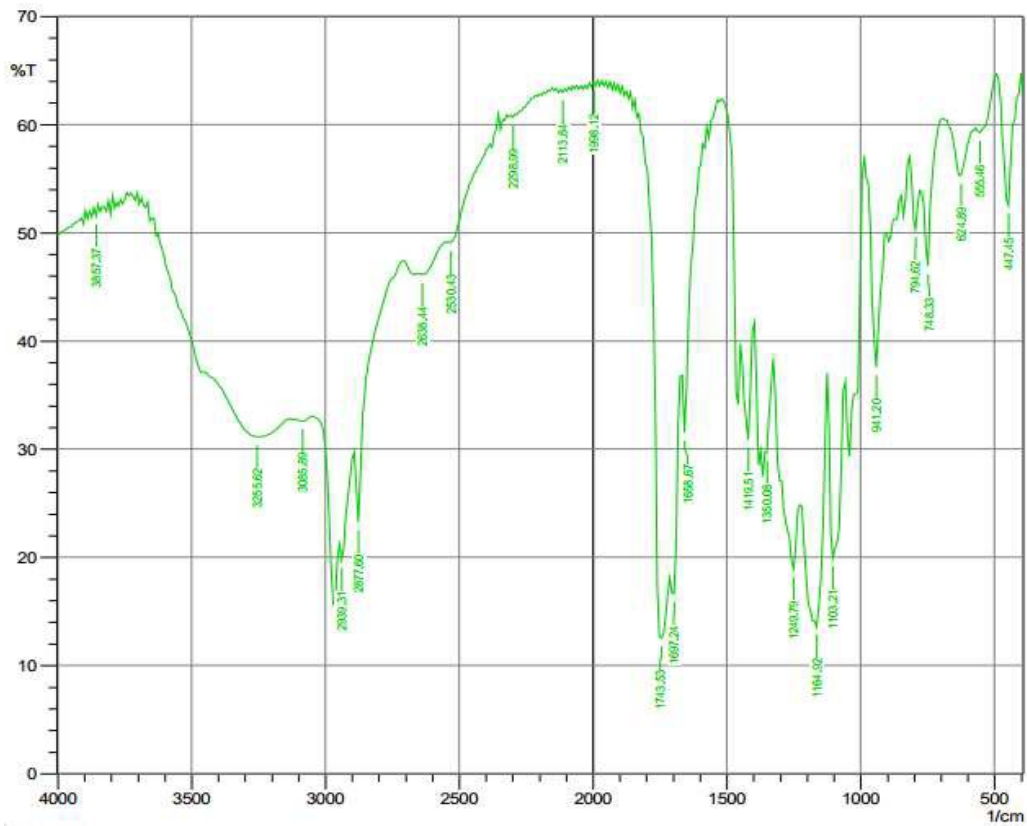


Fig.2 FTIR spectrum of TBS.

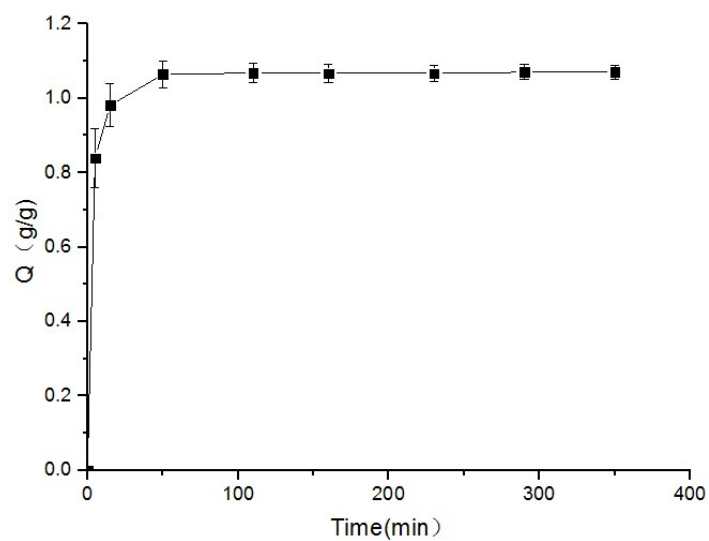


Fig. 3 The variation of the drug-loading capacity (Q) of resin versus time during the TBSS-IER preparation.

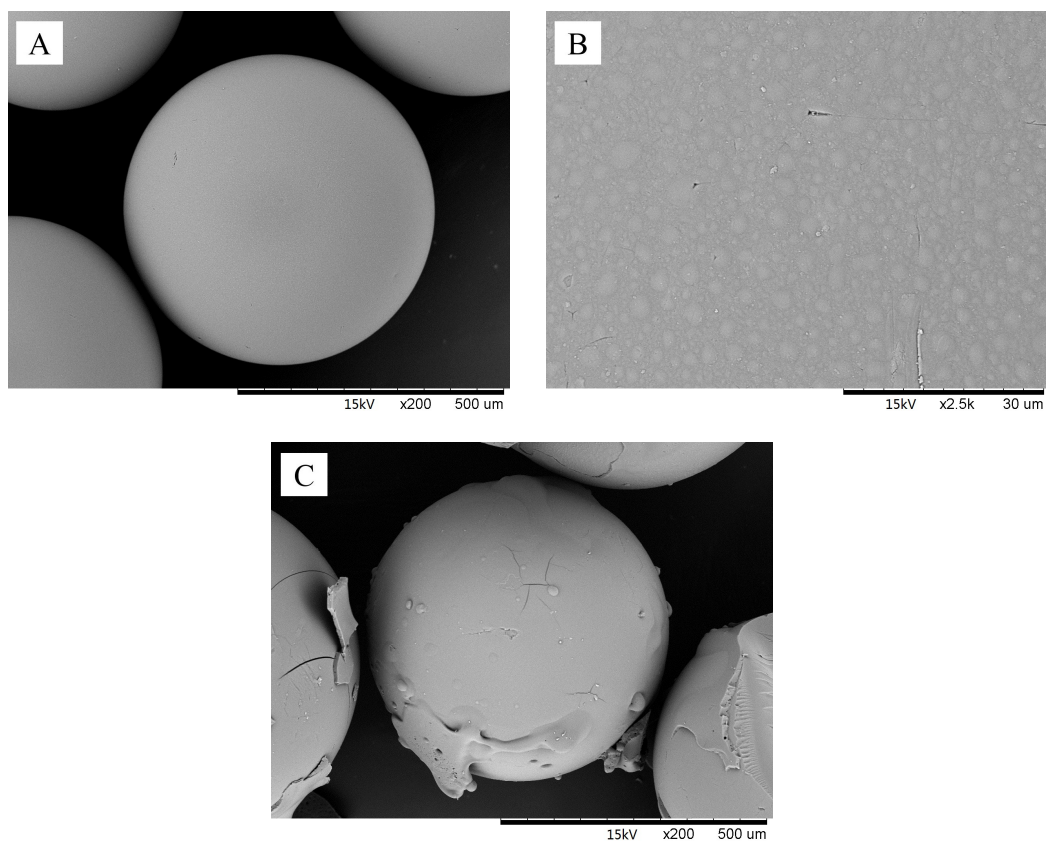


Fig. 4 SEM images of TBSS-IER (A), the surface morphology of TBSS-IER (B) and TBSS-DRM (C).

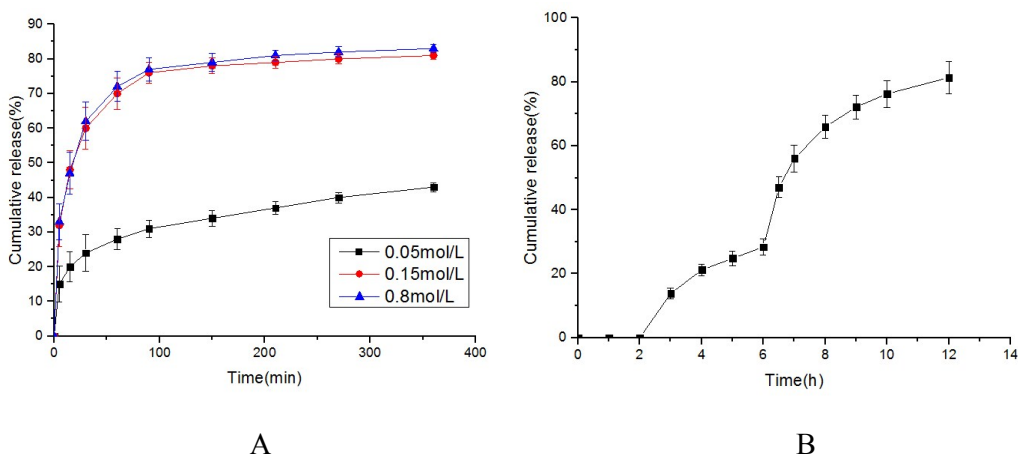


Fig. 5 The *in vitro* release behavior of TBSS-IER in three NaCl solutions of different concentrations (0.05 mol/l, 0.15 mol/l and 0.80 mol/l) (A) and TBSS-DRM in release medium with different pH values (B). For figure B, The experiment was successively conducted at pH 1.2 (from 0 to 2 h), pH 6.8 (from 3 to 6 h) and pH 7.4 (from 7 to 10 h).

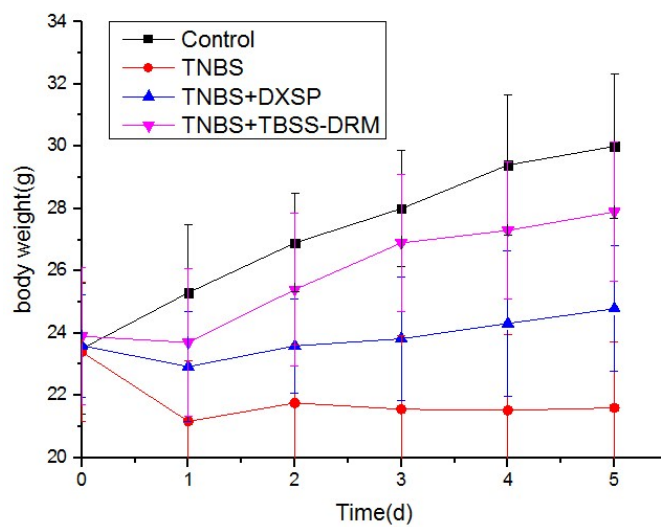


Fig. 6 The influence of TBSS-DRM and DXSP on the body weight changes of mice.

Data are shown as mean \pm SD, n=15.

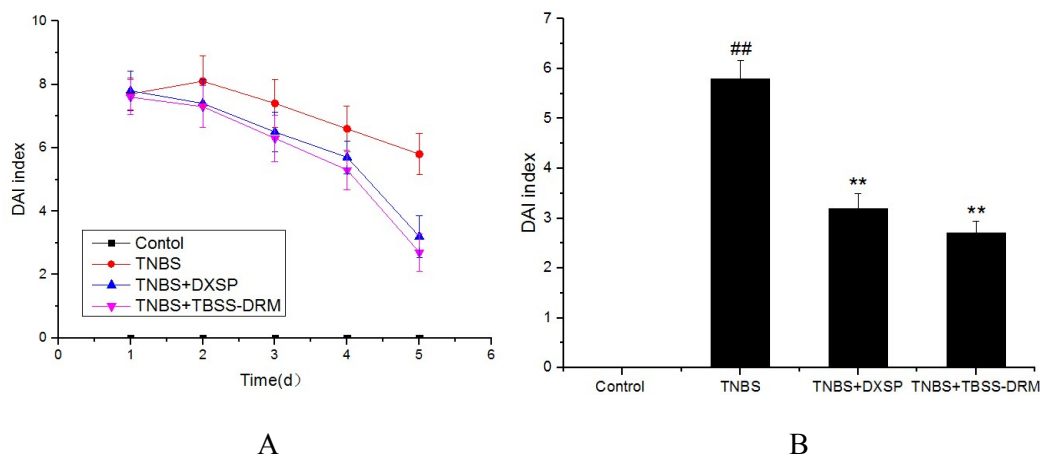


Fig. 7 The influence of TBSS-DRM and DXSP on the variation of DAI index of mice (A) and the influence of TBSS-DRM and DXSP on the ultimate DAI index of mice (B). ^{#,*}Mean values with different superscript symbols were significantly different. ^{##} $p < 0.01$ compared to control group; ^{**} $p < 0.01$ compared to TNBS group. Data are shown as mean \pm SD, $n = 15$. *Control* control group, *TNBS* TNBS group, *DXSP* DXSP p.o. group, *TBSS-DRM* TBSS-DRM p.o. group.

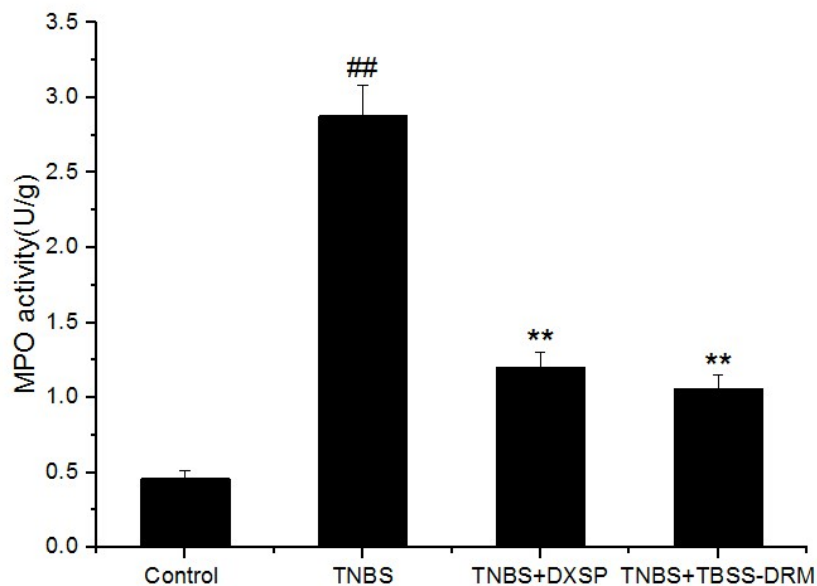


Fig. 8 The influence of TBSS-DRM and DXSP on the activity of MPO in the colon tissue of mice. #,*Mean values with different superscript symbols were significantly different. ## $p < 0.01$ compared to control group; ** $p < 0.01$ compared to TNBS group. *Control* control group, *TNBS* TNBS group, *DXSP* DXSP p.o. group, *TBSS-DRM* TBSS-DRM p.o. group.

Tables**Table 1.** The assay criteria of *o*-benzidine to determine the fecal occult blood of mice.

Results	Phenomenon
Normal	No color occurred after adding reagents for 2 min
Occult blood+	Light blue occurred at first, then turn blue after adding reagents for 10 s
Occult blood++	Light blue occurred at first, then turn brown after adding reagents
Occult blood+++	Brown occurred immediately after adding reagents

Graphical abstract